Light-shift-induced level crossing and resonatorless optical bistability in sodium vapor

T. Ackemann, A. Heuer, Yu. A. Logvin,* and W. Lange
Institut für Angewandte Physik, Westfälische Wilhelms-Universität Münster, Corrensstraße 2/4, D-48149 Münster, Federal Republic of Germany
(Received 19 March 1997)

It is demonstrated experimentally and theoretically that a light-shift-induced level crossing in an oblique magnetic field results in a nonmonotonous dependency of the transmission of a sodium vapor cell on the input power. If feedback by a single plane mirror is added, bistability of the transmission and of the beam profile (resonatorless transverse optical bistability) is observed. The origin of the bistable behavior and the parameter dependencies is explained by the properties of the homogeneous solution. Numerical simulations with a Gaussian incident beam reproduce well the switching behavior of the beam profile found in the experiment. [S1050-2947(97)06209-4]

PACS number(s): 42.65.Sf, 42.65.Pc, 32.80.Bx

I. INTRODUCTION

The creation of population differences between atomic or molecular levels is at the heart of most optical nonlinearities in gases. Examples are the population differences between the ground and the electronically excited state, or between vibrational, hyperfine, and Zeeman sublevels. The refractive index or the absorption coefficient change *monotonously* with increasing light intensity and show typical saturation behavior. In general, however, the interaction with the laser field alone or with the laser field and additional external magnetic and/or electric fields will not only affect the population of the states but can also create a coherent coupling between the sublevels of the upper or the lower state of the transition under consideration. This latter coupling is resonantly enhanced if the levels involved are degenerate, and therefore all mechanisms that affect this degeneracy are expected to influence strongly the nonlinearity. Such an effect, which is intrinsically present in the light-matter interaction, is the level shift caused by a detuned light field [1]. In particular, many widespread schemes for investigating nonlinear effects in atomic vapors involve Zeeman sublevels of the ground state since the population difference is rather long lived and thus significant nonlinearities can be obtained at rather low laser intensities (optical pumping [2]). The basic phenomenon that the light shift has some influence on optical pumping, has been recognized by several authors [3–7]. We will demonstrate that under certain conditions the combined effect of the light-shift, the optical pumping, and the interaction with an external magnetic field can be very drastic: they lead to a *nonmonotonous* dependence of the transmission on the input intensity. This behavior will be shown to be the result of a light-shift-induced level crossing. It gives rise to the possibility of *optical bistability* (OB) [8,9] in the situation of feedback by a *single* mirror.

OB does not only occur in nonlinear resonators [10], but can also be produced by other mechanisms such as e.g., intrinsic light-atom coupling [11] or a polarization instability. Using sodium vapor, bistability between different polarization states has been demonstrated in counterpropagating beams [12] and in a single-mirror setup [13]. In the cases in which the polarization state of the input field did not change and therefore a quasiscalar treatment was applicable, OB in atomic vapors in single-mirror setups was due to self-focusing effects and the resulting saturation of the medium [14,15]. In contrast it is due to the internal degrees of freedom provided by the Zeeman sublevels in our experiment. Although focusing effects are still observed, the OB occurs independently of the focusing or defocusing properties of the sodium vapor and is therefore possible with plane waves in principle. In the Gaussian beam used in the experiment the abrupt change in transmission is accompanied by a change in the beam profile, which also shows hysteresis. This means that *transverse optical bistability* is observed. This phenomenon is known to exist also in nonlinear resonators [16–18] but it is much less studied than conventional OB.

II. EXPERIMENT

The experiment has been carried out using the setup schematically presented in Fig. 1. A frequency-stabilized cw dye laser is detuned slightly below the Na-D_1 resonance. An

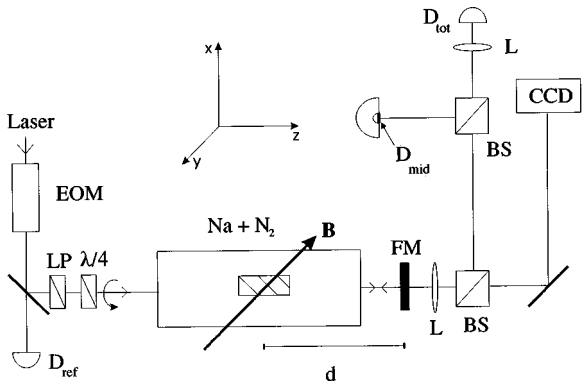

FIG. 1. The experimental setup. EOM: electro-optic-modulator, LP: linear polarizer, λ/4 quarter-wave plate, FM: feedback mirror; L: lens; BS: beam splitter, D_{ref}, D_{mid}, and D_{tot}: photodiodes and charge-coupled-device camera.

*Permanent address: Institute of Physics, Belarusian Academy of Sciences, Scaryna Ave. 70, 220072 Minsk, Belarus.

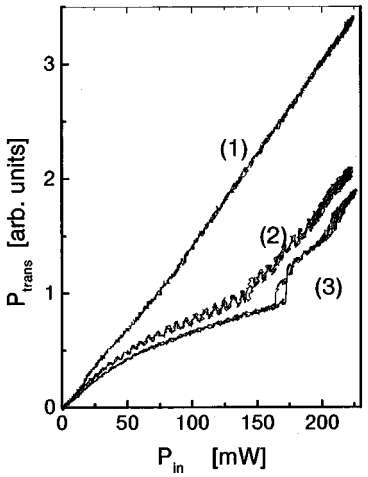

FIG. 2. Transmitted power P_{trans} (proportional to the signal of D_{tot}) in dependence of the input power (P_{in}). Parameters: Larmor frequency corresponding to the longitudinal component of the magnetic field $\Omega_z = -2\pi \times 78$ kHz, detuning $\Delta = -11.2$ GHz, sodium particle density $N \approx 0.85 \times 10^{14}$ cm^{-3}, distance between cell center and mirror $d = 320$ mm, Larmor frequency corresponding to the transverse component $\Omega_x \lesssim 2\pi \times 3$ kHz [curve (1)], $\Omega_x = 2\pi \times 9$ kHz [curve (2)], $\Omega_x = 2\pi \times 17$ kHz [curve (3)].

electro-optical modulator is used for intensity control. The beam is spatially filtered by transmitting it through a single mode fiber to remove beam inhomogeneities that might induce filamentation. After that it is enlarged and collimated ($1/e^2$ radius of irradiance w_0 being 1.4 mm). Due to the rather large beam radius the change of the beam radius due to self-lensing is hardly noticeable within the medium (the lens power is inversely proportional to the beam radius in a first approximation, cf., e.g., [19]). Finally, the beam is converted to circular polarization and injected into a sodium cell. Sodium vapor in a nitrogen buffer gas atmosphere at a pressure of 300 mbar is contained in a glass tube of 8 mm diameter, with the length of the heated zone being 15 mm. We apply an external magnetic field, which is generated by a system of three pairs of Helmholtz coils. A feedback mirror with a reflectivity $R = 91.5\%$ is placed at a distance $120 \leqslant d \leqslant 320$ mm behind the cell center. The exit face of the medium is imaged by a lens onto a charge-coupled-device camera to obtain the near field intensity distribution. The photodiode D_{tot} yields a signal that is proportional to the total transmitted power P_{trans}. An additional photodiode D_{mid}, positioned in the image plane, measures the transmitted power in the central part of the beam only (radius of the diode $r = 0.15 w_0$, homogeneity of intensity 5%).

Figure 2 shows the total power of the transmitted beam for three values of the transverse magnetic field and a suitable combination of the other parameters (see below), which is observed when the power of the incident light is scanned adiabatically (scan time 2 s). If the transverse magnetic field is nearly compensated, then we observe nearly linear behavior of the transmitted power [Fig. 2 curve (1)]. This indicates a very high saturation of the vapor. The residual stray fields are of the order of 0.5 μT, corresponding to a Larmor frequency of 3–4 kHz. We characterize the magnetic field by giving the corresponding Larmor frequency in the following. If a small transverse magnetic field is applied intentionally, then the absolute transmitted power decreases and the shape of the transmission curve becomes clearly nonlinear [Fig. 2 curve (2)]. For $P_{\text{in}} \gtrsim 30$ mW the slope of the characteristic flattens and at about 140 mW there is a bend and finally the slope increases again. If the transverse magnetic field is further increased, the transmitted power shows an abrupt raising of switching type at about $P_{\text{in}} = 170$ mW [Fig. 2, curve (3)]. After this point the output power increases again continuously with increasing input power. At $P_{\text{in}} = 200$ mW we observe an additional pronounced change of the transmission, but no switching. Scanning P_{in} down reproduces the curve except in the domain of abrupt change, where we observe downward switching at $P_{\text{in}} = 162$ mW. As a result hysteretic behavior is found in the transmission characteristic; i.e., there is optical bistability.

The conditions for the occurrence of optical bistability are a weak transverse magnetic field ($B_x \approx 5\mu$ T) and a stronger longitudinal B_z applied parallel to the direction of the backward beam, when σ_+ polarized light detuned below the Na-D_1 resonance is used. (The direction of the forward beam is chosen as the axis of quantization.) Inverse detuning or replacing the σ_+ polarization by σ_- requires the opposite direction of B_z. Without transverse magnetic field optical bistability is never observed. Its direction in the x-y plane may be arbitrarily chosen, although its strength determines the system behavior crucially, i.e., even very weak stray fields produce strong changes. As a matter of fact, this is the reason for the observed ripples on the presented data. OB as well as the hysteretic change in beam profile, which is discussed below in Sec. IV, occur on both sides of the resonance in a similar manner. We will confine ourselves to the low frequency side for a systematic presentation and comparison with the theory since beam shaping effects within the medium can be expected to be somehow smaller.

The change of slope in the signal in Fig. 2 at about 30 mW indicates that the normalized total transmission $T = P_{\text{trans}}/P_{\text{in}}$ does not only saturate, but *decreases* with *increasing* input power. This can be deduced from Fig. 3, which presents contour lines of equal transmission in the plane of control parameters. Figure 3 reveals a high transmission (i.e., high saturation of the medium) already for small P_{in}. Increasing P_{in} at constant B_z yields a gradual decrease of T up to a certain point of sudden change. Afterwards T increases monotonously until the medium is completely saturated. The point of sudden change moves to higher P_{in} with increasing $|B_z|$. The nearly parallel isolines indicate the ability of the input power to compensate the influence of the longitudinal magnetic field, and vice versa. Actually the development of a transmission dip is also observed, when the longitudinal magnetic field is scanned and P_{in} is kept fixed.

A certain threshold value of the particle density N is required to obtain optical bistability. When N is increased, the initially symmetric dip deepens and becomes asymmetric. At about $N \approx 0.3 \times 10^{14}$ cm^{-3} (for the parameters considered here) the system shows optical bistable behavior.

It has to be stressed that a dip in the transmission curve also exists without feedback by the mirror, but bistability does not occur in that case (Fig. 4). Furthermore, the figure illustrates that the transmission curve has the usual monotonous characteristic of a saturable medium, if the direction of

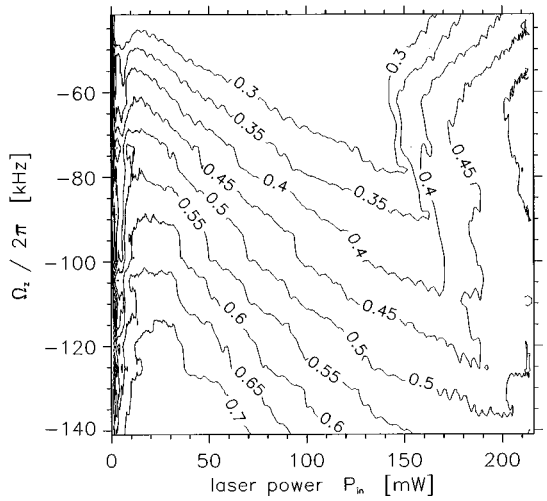

FIG. 3. Contour lines of equal total transmission T in dependency of the input power P_{in} and the longitudinal Larmor frequency Ω_z. The graph was created from 20 data sets for different values of Ω_z. Each of the data sets consists of 1150 points obtained by adiabatically increasing the input power at constant Ω_z. Parameters as in Fig. 2, but $\Omega_x = 2\pi \times 14$ kHz.

the longitudinal magnetic field is reversed.

III. THEORETICAL MODEL

For a theoretical description of the experiment, following the approach [20], we treat the sodium D_1 line as a homogeneously broadened $J = 1/2 \rightarrow J' = 1/2$ transition. In the case under consideration the nonlinear optical properties of the medium are determined by the $J = 1/2$ ground state, which is split into two Zeeman sublevels in the external magnetic field. Circularly polarized (σ_+) light propagating along the z direction creates a population difference w (orientation) between the sublevels. Let us define a Bloch vector $\boldsymbol{m} = (u, v, w)$ whose components are proportional to the expectation values of the resulting magnetic moment. Its evolution is described by

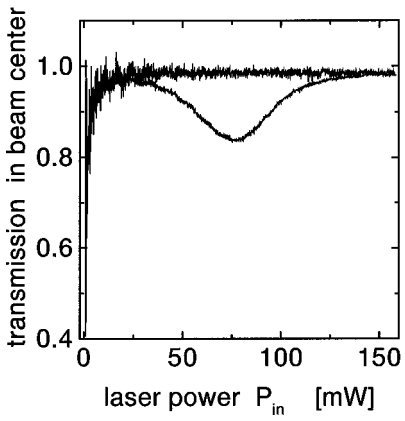

FIG. 4. Transmission in beam center (normalized signal of D_{mid}) as a function of input power without feedback by the mirror. Parameter: $\Omega_z = -2\pi \times 177$ kHz (lower curve), $\Omega_z = 2\pi \times 177$ kHz (upper curve), $\Delta = -10$ GHz, $N \approx 2.8 \times 10^{12}$ cm^{-3}, $\Omega_x = 2\pi \times 27$ kHz. The curves have been averaged over 20 runs.

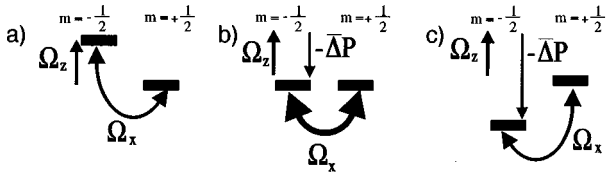

FIG. 5. The light-shift-induced level crossing. The direction of the arrow indicates the direction of the movement of the level with $m_J = -1/2$. (a) Strong splitting of the Zeeman sublevels caused by the longitudinal external field without a light field. (b) The light shift compensates the longitudinal magnetic field exactly. (c) In a very strong light field the degeneracy is lifted again.

$$\partial_t \boldsymbol{m} = -(P - D\Delta_\perp + \gamma)\boldsymbol{m} - \boldsymbol{m} \times \boldsymbol{\Omega} + \hat{\boldsymbol{e}}_z P. \qquad (1)$$

The terms in brackets describe losses of orientation depending on the optical pump rate P [proportional to the intensity, cf. Eq. (4) below for the exact relationship], diffusion of the oriented particles (D is the diffusion constant and $\Delta_\perp = \partial^2/\partial_x^2 + \partial^2/\partial_y^2$ the transverse Laplacian) and their collisions with buffer gas atoms ($\gamma \approx 6\ \mathrm{s}^{-1}$). The second term describes the precession of $\boldsymbol{m}$ around the effective magnetic field vector $\boldsymbol{\Omega} = (\Omega_x, 0, \Omega_z - \overline{\Delta P})$. $\boldsymbol{\Omega}$ does not only contain the Larmor frequencies produced by the Cartesian components of the magnetic field $(\Omega_x, 0, \Omega_z)$, but also the light-intensity-dependent term $\overline{\Delta P}$ [with $\overline{\Delta} = 2\pi\Delta/\Gamma_2$ being the detuning normalized to the homogeneous linewidth half-width at half maximum (HWHM) Γ_2]. Finally, the third term describes the creation of orientation due to optical pumping. Assuming the incident field to be a plane wave we find the steady state orientation

$$w = \frac{P}{\gamma + P}\left(1 - \frac{\Omega_x^2}{(\Omega_z - \overline{\Delta P})^2 + (\gamma + P)^2 + \Omega_x^2}\right). \qquad (2)$$

As long as there is no feedback (i.e., without a mirror) the pump rate is given by the pump rate P_0 produced by the incident field alone, and the dependence of w on P can easily be discussed. For very low P_0 the medium is strongly saturated, since γ is very small and the second term in parentheses is small for $\Omega_z \gg \Omega_x$. Without a magnetic field the medium would stay in this saturated condition independent of any further increase of P_0. However, the second term in the parentheses of Eq. (2) creates a nearly symmetric resonance-like dip in the $w(P_0)$ characteristic as shown in Fig. 6, if the transverse magnetic field is nonvanishing. This resonance results from a light-shift-induced level crossing, which is illustrated in Fig. 5. For vanishing P_0 the levels are split by the external magnetic field [Fig. 5(a)]. In this case the (coherent) coupling of the Zeeman sublevels by the transverse magnetic field is weak. Thus a large orientation is produced even at small values of P_0, which do not yet influence the level splitting significantly. For a suitable choice of the signs of Ω_z and $\overline{\Delta}$ the splitting decreases if P_0 increases. Therefore the strength of the coupling increases and the orientation is diminished. The minimum of orientation is achieved, if light shift and external longitudinal field equalize each other [Fig. 5(b)]. Overcompensation of the external field by the light shift creates again a splitting of the sublevels [Fig. 5(c)] and as a consequence the orientation increases again.

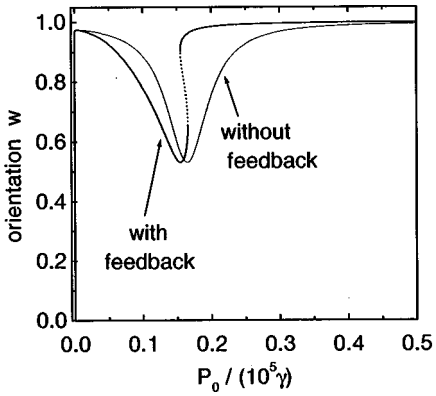

FIG. 6. Orientation w of the probe in dependence of the pump rate P_0. The graph shows w in the case with and without feedback. It is monotonously connected to the transmission by Eq. (6).

Modifications of optical pumping in the ground state by light-shift effects have been discussed by Röhricht *et al.* [6]. In zero magnetic field a light-shift-induced resonance was found earlier in fluorescence experiments in barium vapor. It was named *optical Hanle effect* [21,22]. Here a more general phenomenon is encountered, which might be called *light-shift-induced level crossing.*

In the analysis of the case with feedback the action of the medium on the optical field and the propagation of the field to the mirror (reflectivity R) and back have to be considered.

If the diffraction within the medium is neglected, the connection between the incident (E_0) and transmitted (E_t) field is given by

$$E_t = E_0 e^{-i\chi_{nl} kl/2}. \tag{3}$$

χ_{nl} is the complex susceptibility of the sodium vapor, k is the wave number, l is the length of the heated zone. The backward field $E_b = \sqrt{R}\exp(-id/k\Delta_\perp)E_t$ is obtained from the paraxial wave equation in free space. The resulting pump rate

$$P = \frac{3}{16}(|E_0|^2 + |E_b|^2)\frac{|\mu_e|^2}{4\hbar^2 c\epsilon_0 \Gamma_2(\overline{\Delta^2}+1)} \tag{4}$$

is taken to be proportional to the sum of the intensities, in the manner of Firth's model [23].

In Eq. (4) μ_e is the dipole matrix element of the atomic transition and the factor of 3/16 gives a rough account for the reduction of pump efficiency due to the hyperfine splitting [24]. The orientation w, calculated from Eq. (1), is inserted into the formula for the complex nonlinear susceptibility of the medium

$$\chi_{\rm nl} = -\frac{N|\mu_e|^2}{2\hbar\epsilon_0\Gamma_2}\frac{\overline{\Delta}+i}{\overline{\Delta^2}+1}(1-w) \equiv \chi_{\rm lin}(1-w). \tag{5}$$

Here N is the particle density of the sodium vapor. The imaginary part of Eq. (5) yields the small signal absorption coefficient $\alpha_0 = -\,\mathrm{Im}(\chi_{\rm lin})/2$, which is connected to the transmission by

$$T = \frac{|E_{\rm tr}|^2}{|E_0|^2} = e^{-2\alpha_0(1-w)l}. \tag{6}$$

With a feedback mirror ($R>0$) the effective pump rate is the sum of P_0 and P_b. Obviously, minimum orientation is achieved at lower pump rate P_0 (Fig. 6). In addition, positive feedback causes the resonance to bend, and can lead to the appearance of a three valued interval that corresponds to optical bistability. This curve has the typical shape of a nonlinear resonance [25].

The dependencies of both the appearance and the pump threshold of optical bistability on the parameters transverse and longitudinal magnetic field (i.e., Fig. 3) and particle density are found to be in qualitative agreement with the plane-wave theory.

IV. DETAILED COMPARISON OF EXPERIMENTAL AND THEORETICAL RESULTS

A quantitative comparison requires one to take into account the Gaussian intensity distribution of the input beam. In the analysis we integrate Eq. (1) numerically on a Cartesian grid (256×256) using a Gaussian distribution $[P_0(r) = (2P_{\rm in}/\pi w_0^2)\exp(-2r^2/w_0^2)]$ for the incident beam. The change in field distribution due to propagation to the mirror and back is calculated in Fourier space.

Figure 7 shows the transmission T versus the input power, obtained in the experiment [Fig. 7(a)], the numerical simulations [Fig. 7(b)], and the analytical plane-wave treatment [Fig. 7(c)]. [In the case of Figs. 7(a),(b), T was measured in the center of the Gaussian beam.] In Fig. 7(b) we used two different scales for the input power: the units of mW are adequate in comparing the results of the simulations with the experiment, while the use of the $P_0(0)/\gamma$ allows one to establish the connection between the numerical and analytical results. One can see that each graph shows the same qualitative behavior. Strong saturation of the medium is found for small pump rates. After this interval of saturation, an increase of the pump results in a decrease of the transmission until the minimum is reached. After the minimum, the characteristics in Figs. 7(a),(b) show an abrupt switching to a high transmission state. The switching process is hysteretic. In the analytical curve in Fig. 7(c) the switching points correspond to the saddle-node bifurcation points in the domain of the ''nonlinear resonance.'' For a Gaussian input beam we observe another interval of sharply rising transmission for both experiment and simulation [cf. also the behavior of the total transmitted power, curve (3) in Fig. 2]. As shown in our previous works [7,26], the system under consideration might exhibit spontaneous symmetry breaking and pattern formation. While we observe little pattern formation in the experiment (for the chosen parameters), the tendency to pattern formation is stronger in the numerical simulations. This is the origin of the wriggly behavior of the transmission curve between 60 and 110 mW in Fig. 7(b). A standard linear stability analysis of the system [26] shows indeed that the homogeneous state in question is unstable against inhomogeneous perturbations [Fig. 7(c)].

In the experiment as well as in the numerical simulations the switching is accompanied by a sudden change of the

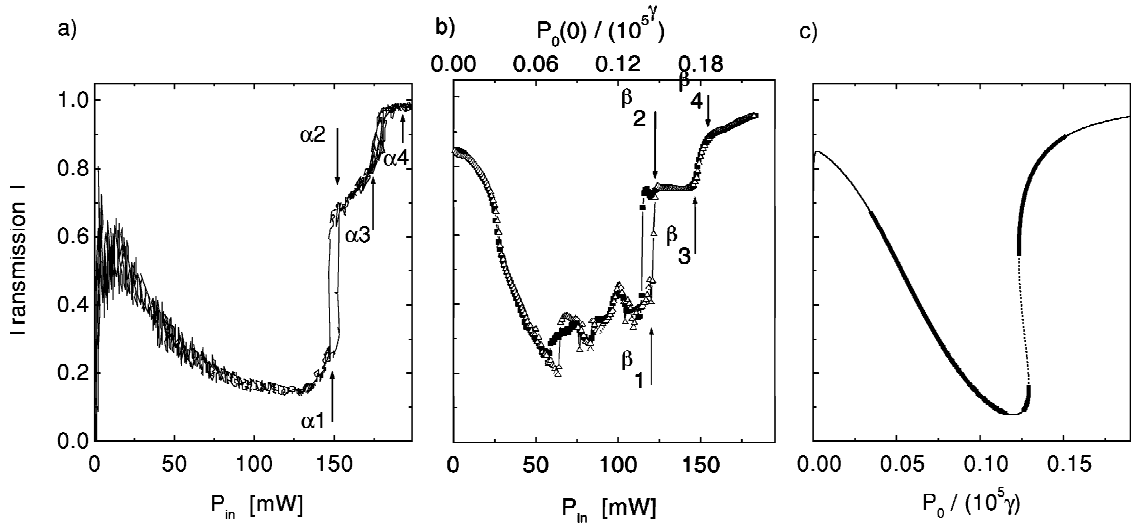

FIG. 7. Transmission T in dependence of the input power P_{in}. The parameters are the same as in Fig. 2 but $\Omega_x = 2\pi \times 14$ kHz. The arrows mark the points for which the near field distribution is shown in Fig. 8. (a) The experimental result, (b) the result of the numerical simulation, (c) the homogeneous solution [Eq. (2)]. The bold lines of the plot show the areas in which the linear stability analysis yields an instability against inhomogeneous perturbations.

intensity profile in the beam center, as visible in Fig. 8 and even better in the cross sections in Fig. 9. Before switching [Fig. 8(α1), (β1), and Fig. 9(α1), (β1)] one observes a needlelike peak in the beam center that is surrounded by a ring of small intensity. Additional holelike intensity minima are present in the beam wings. As mentioned above, these intensity minima are due to spontaneous pattern formation and are more pronounced in the simulations. The switching itself is accompanied by a change of the intensity profile to a columnlike structure [Fig. 8(α2), (β2) and Fig. 9(α2), (β2)]. Since the shape of the transverse profiles on the high transmission branch of the bistable region is the same as in Fig. 8(α2), (β2), different intensity distributions [Fig. 8(α1) and (α2), (β1), and (β2)] are obtained for the same input power. Obviously the system shows transverse optical bistability in this part of the transmission characteristic [17,18]. The radius of the column increases if the power is increased further. This expansion process goes on continuously, but the change is rather large for the pump value at which also the transmission shows the second, pronounced rise described above [Fig. 7(a), $P_{\mathrm{in}} \approx$ 180 mW corresponding to the transition between 8(α3) and 8(α4); an analogous transition takes place in Fig. 7(b) at $P_{\mathrm{in}} \approx$155 mW. As apparent from the cross sections [Figs. 9(α2)–9(α4)] there is a ''spatial overshooting'' in the edges of the columns and there are many small rings in the inside. These structures show a resemblance to the rings generated by the Fresnel diffraction at a circular aperture. Indeed the very inhomogeneous orientation profile, which is present in the vapor after the switching process took place in beam center, can be regarded as a *self-induced* aperture. Since the interaction zone has a length of 15 mm in the experiment, some diffraction of the light beam takes place already in the medium. This diffraction inside the medium, however, was not taken into account in the simulations. This accounts for the deviations between the experimental and the numerical results, while the overall similarity between the experimental and numerical results in Figs. 8 and 9 is evident. The agreement of the absolute value of the switching threshold in experiment and simulation within 20% can be judged to be very satisfactory, taking into account that inside the medium the depletion of the beams by absorption is neglected and the hyperfine coupling is only very roughly accounted for.

V. CONCLUSION

We demonstrated that a light-shift-induced level crossing provides a mechanism for resonatorless optical bistability in

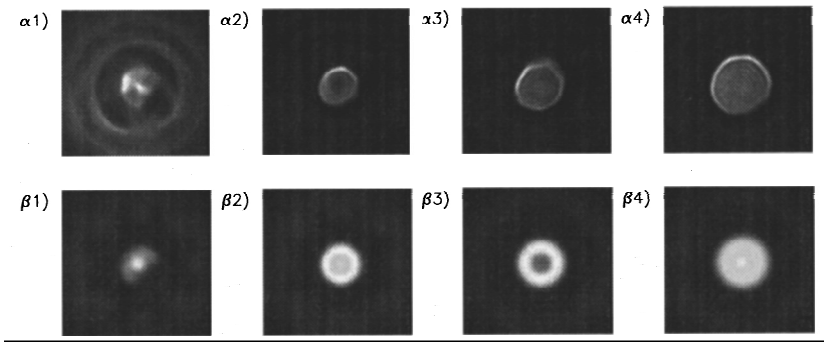

FIG. 8. Near field intensity distributions in the vicinity of optical bistability. Upper row: Experiment. Lower row: simulations. The location of the patterns on the transmission curves is indicated in Fig. 7. The frames have a size of 2.4 × 2.4 mm.

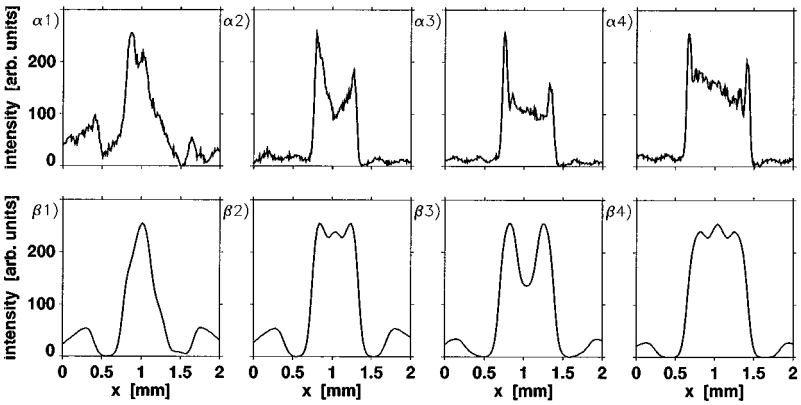

FIG. 9. Cross sections of the patterns in Fig. 8 through the beam center along a horizontal line.

an atomic vapor, which in principle does not depend on self-focusing or defocusing effects. Since a single-mirror device is experimentally preferable to a resonator, the system might be suited to study the mechanism that determines the spatial extent of the highly transmitting state and the possibility of localized states in detail. Moreover, all ''traditional'' nonlinear optical experiments are expected to be influenced greatly by a nonmonotonous characteristic. For the case of degenerate four-wave mixing this was recently observed by [4], although the connection to an induced level crossing was not worked out explicitly. The possibility to tailor the shape of the nonlinear characteristic by simply adjusting an external magnetic field is also considered to be useful in a variety of nonlinear optical experiments. In particular, we demonstrated that it facilitates the investigation of optical patterns and general features of pattern formation (e.g., the transition between positive and negative hexagons [7]) that cannot be obtained in Kerr-like media.

[1] C. Cohen-Tannoudji, Ann. Phys. (N.Y.) **7**, 423 (1962).
[2] A. Kastler, J. Opt. Soc. Am. **47**, 460 (1957).
[3] C. Boden, M. Dämmig, and F. Mitschke, Phys. Rev. A **45**, 6829 (1992).
[4] M. Schiffer, E. Cruse, and W. Lange, Phys. Rev. A **49**, R3178 (1994).
[5] A. Gahl, J. Seipenbusch, A. Aumann, M. Möller, and W. Lange, Phys. Rev. A **50**, R917 (1994).
[6] B. Röhricht, P. Eschle, C. Wigger, S. Dangel, R. Holzner, and D. Suter, Phys. Rev. A **50**, 2434 (1994).
[7] T. Ackemann, A. Yu. Logvin, A. Heuer, and W. Lange, Phys. Rev. Lett. **75**, 3450 (1995).
[8] A. Szöke, V. Daneu, J. Goldhar, and N. A. Kurnit, Appl. Phys. Lett. **15**, 376 (1969).
[9] H. M. Gibbs, S. L. McCall, and T. N. C. Venkatesan, Phys. Rev. Lett. **36**, 1135 (1976).
[10] H. M. Gibbs, *Optical Bistability: Controlling Light with Light* (Academic, New York, 1985).
[11] D. A. B. Miller, A. C. Gossard, and W. Wiegmann, Opt. Lett. **9**, 162 (1981).
[12] D. J. Gauthier, M. S. Malcuit, A. L. Gaeta, and W. Boyd, Phys. Rev. Lett. **64**, 1721 (1990).
[13] T. Yabuzaki, T. Okamoto, M. Kitano, and T. Ogawa, Phys. Rev. A **29**, 1964 (1984).
[14] J. E. Bjorkholm, P. W. Smith, W. J. Tomlinson, and A. E. Kaplan, Opt. Lett. **6**, 345 (1981).
[15] M. LeBerre, E. Ressayre, A. Tallet, K. Tai, and H. M. Gibbs, IEEE J. Quantum Electron. **21**, 1404 (1985).
[16] W. J. Firth and E. M. Wright, Opt. Commun. **40**, 233 (1982).
[17] N. N. Rosanov, Spectrosc. Lett. **1840**, 130 (1991).
[18] J. Nalik, L. M. Hoffer, G. L. Lippi, Ch. Vorgerd, and W. Lange, Phys. Rev. A **45**, R4237 (1992).
[19] M. Sheik-Bahae, A. A. Said, D. J. Hagan, M. J. Soileau, and E. W. Van Stryland, Opt. Eng. (Bellingham) **30**, 1128 (1991).
[20] F. Mitschke, R. Deserno, W. Lange, and J. Mlynek, Phys. Rev. A **33**, 3219 (1986).
[21] C. Delsart, J. -C. Keller, and V. P. Kaftanjian, Opt. Commun. **32**, 406 (1980).
[22] V. P. Kaftanjian, C. Delsart, and J.-C. Keller, Rev. Phys. **23**, 1365 (1981).
[23] G. D'Alessandro and W. J. Firth, Phys. Rev. A **46**, 537 (1992).
[24] M. Möller and W. Lange, Phys. Rev. A **49**, 4161 (1994).
[25] L. B. Landau and E. M. Lifshitz, *Mechanics* (Pergamon, Oxford, 1976).
[26] W. Lange, Yu. A. Logvin, and T. Ackemann, Physica D **96**, 230 (1996).